JOURNAL OF Applied Polymer SCIENCE

Synthesis of poly(*N*-isopropylacrylamide) by distillation precipitation polymerization and quantitative grafting on mesoporous silica

Sushilkumar A. Jadhav,[1] Valentina Brunella,[1] Ivana Miletto,[1,2] Gloria Berlier,[1] Dominique Scalarone[1]

[1]Department of Chemistry and NIS Research Centre, University of Torino, Italy

[2]Department of Science and Technological Innovation, Università del Piemonte Orientale, Alessandria, Italy

Correspondence to: S. A. Jadhav (E-mail: sushil.unige@gmail.com)

ABSTRACT: In this work, syntheses of thermoresponsive poly(*N*-isopropylacrylamide) (PNIPAM) with different molecular weights were carried out in ethanol by distillation precipitation polymerization (DPP) technique. The synthesized polymers were fully characterized by attenuated total reflection Fourier-transform infrared (ATR-FTIR) spectroscopy, nuclear magnetic resonance spectroscopy, and size exclusion chromatography techniques. The lower critical solution temperatures of the polymers were determined with differential scanning calorimetry. A simple and versatile method for the *in situ* synthesis and grafting of PNIPAM on mesoporus silica nanoparticles (MSNs) with improved control over quantitative grafting is devised. The PNIPAM grafted MSNs were characterized with ATR-FTIR, thermogravimetric analysis, transmission electron microscopy, and dynamic light scattering analyses. From the results obtained it is showed that quantitative grafting of PNIPAM on MSNs from 1 to 20% by weight can be tuned by manipulating the *in situ* DPP reaction conditions. © 2016 Wiley Periodicals, Inc. J. Appl. Polym. Sci. **2016**, *133*, 44181.

KEYWORDS: nanoparticles; nanowires and nanocrystals; radical polymerization; stimuli-sensitive polymers; surfaces and interfaces

Received 8 April 2016; accepted 12 July 2016

DOI: 10.1002/app.44181

INTRODUCTION

Poly(*N*-isopropylacrylamide) (PNIPAM) is a water soluble thermoresponsive polymer which shows a typical coil-to-globule transition at its lower critical solution temperature (LCST) which is around 31–32 °C.[1–3] Synthesis of linear, block, and random copolymers of PNIPAM and PNIPAM-grafted hybrid particles or surfaces were carried out by various polymerization techniques which include atom transfer radical polymerization (ATRP),[4–6] radical polymerization,[7–10] and photopolymerization.[11] Each of these techniques has its advantages and can yield PNIPAM with different properties such as molecular weight (M_w) and dispersity. When it comes to the grafting of polymers such as thermoresponsive PNIPAM or its various copolymers on nanoparticles of different materials the choice of the polymerization technique becomes crucial. The polymerization technique chosen and the quantitative grafting both play important roles to tune the properties of the resulting polymer grafted particles. In the case of porous particles the reversible thermosensitive transition of PNIPAM chains from extended coils to compact globules above its LCST applies a pore opening and closing mechanism to the pores, which is very interesting for controlled and/or targeted delivery of active molecules and drugs.[12,13] The efficiency of polymer grafting is determined by the polymerization technique and the proper pore opening–closing mechanism is governed both by the effective grafting and quantity of the polymer grafted. Thus the polymerization method should guarantee the polymer formation, its simultaneous grafting inside the pores of the particles and control over the quantitative grafting. All the components of the polymerization reaction mixture, such as solvent, initiator, monomer/s, and the polymerizable group anchored on the particles and their reactivity play an important role in the synthesis of the polymer-grafted particles. For this purpose, distillation precipitation polymerization (DPP) technique provides some advantages as it is a relatively simple technique with a combination of precipitation and radical polymerization and works well with particles of various materials.[14] Some of the interesting reports about DPP include synthesis of monodisperse poly(methacrylic acid) microspheres[15] and synthesis of superhydrophobic fluorinated polystyrene microspheres.[16] Instead reports about polymer grafting on nanoparticles by DPP include polymerization of methacrylic acid on PMMA/TiO_2 composite nanospheres,[17] synthesis of PNIPAM-grafted silica and mesoporous silica

Additional Supporting Information may be found in the online version of this article.

nanoparticles,[18,19] DPP-mediated grafting of poly(4-vinyl benzylchloride) for the generation of chlorine functionalized Fe_3O_4 hybrid composites,[20] synthesis of poly(acrylic acid)-grafted magnetite nanoparticles for the generation of magnetic metal–organic framework nanospheres,[21] preparation of erythromycin molecularly imprinted polymers,[22] synthesis of metronidazole-imprinted polymers,[23] and boronate core–shell polymer nanoparticles for glycoprotein recognition via combined DPP and RAFT media precipitation polymerization.[24] All these examples mentioned show the versatility of DDP technique in synthesis and grafting of various polymers. So although initially DPP technique was reported for the synthesis of microspheres of polymers it is revealed that it also works well for the synthesis and grafting of polymers, especially PNIPAM, on various nanoparticles.[14,19]

Effective polymerization and simultaneous controlled grafting of polymer on surfaces or particles are two important steps in the synthesis of polymer-grafted materials. Control over the polymer grafted on 2D surfaces or particles is of importance as the quantity of polymer grafted plays an important role to tune the properties of the resulting composites, hybrid surfaces, or particles. Hence the reports about controlled grafting of polymers are considered as important technological advancements and there is a constant need of evaluation and suitable modification of existing polymerization techniques for increased control on polymer grafting. In the present work, we report on the synthesis and characterization of PNIPAM homopolymers by DPP in ethanol, on the effect of molecular weight of the synthetized PNIPAMs on their LCST, and on controlled quantitative grafting of PNIPAM on mesoporous silica nanoparticles (MSNs) by careful manipulation of the *in situ* DPP reaction conditions. The synthesized PNIPAM-grafted mesoporous silica particles possess several potential applications in temperature triggered delivery of molecules loaded inside the porous particles.[25] The release (trafficking) of the molecules from the pores can be controlled by the thermosensitive transition of PNIPAM. Besides the synthetic improvements presented in this work on PNIPAM grafting on porous nanoparticles, the results also have a general scope as the controlled quantitative grafting technique can be utilized for the grafting of PNIPAM and its copolymers on micro- or nanoparticles and surfaces of various materials.

EXPERIMENTAL

Materials

N-Isopropylacrylamide (NIPAM), azobisisobutyronitrile (AIBN), tetraethoxysilane (TEOS), cetyltrimethylammonium bromide (CTAB), 1,3,5-trimethylbenzene (TMB), 3-(methacryloxypropyl) trimethoxysilane (MPS) were purchased from Sigma–Aldrich, Italy. All the solvents used for the synthesis were of high purity and used as received. Ethanol was kept on molecular sieves overnight before using for polymerization reaction.

Instruments and Methods

Fourier-transform infrared (FTIR) spectra were recorded on a Perkin Elmer Spectrum 100 in the attenuated total reflectance (ATR) mode with a diamond crystal, using 16 scans per spectrum and a resolution of 4 cm^{-1} and a spectral range of 4000–600 cm^{-1}. Proton nuclear magnetic resonance (NMR) spectra were recorded on a Bruker Avance (200 MHz) NMR spectrometer in deuterated dimethyl sulfoxide (DMSO-d_6) using tetramethylsilane (TMS) as reference.

Size exclusion chromatography (SEC) was performed with a Viscotek modular instrument equipped with a VE 1122 pump, a VE 7510 degasser, manual injection valve, VE 3580 refractive index detector, column oven, and two PLgel 10 μm MIXED-B columns (Polymer Laboratories, UK). *N*,*N*-Dimethylformamide (DMF) (1.0 mL min^{-1}) was used as eluent. Due to the density of DMF, analyses were performed setting the column oven at 70 °C. This allows to keep the backpressure of the system low and to improve the analysis resolution. In DMF, PNIPAM does not show a coil-to globule transition; hence chains are solvated coils also at 70 °C. DMF solutions of the samples (3 mg mL^{-1}) were filtered through 0.45-μm polytetrafluoroethylene (PTFE) membrane filters. Calibration was obtained with poly(methyl methacrylate) (PMMA) molecular weight (M_w) standards.

A differential scanning calorimeter (DSC) Q200 from TA Instruments was used to collect DSC thermograms. DSC scans were performed with closed aluminum pans under nitrogen atmosphere and with a 10 °C min^{-1} heating rate, from 20 °C up to 60 °C. Thermogravimetric analyses (TGA) were carried out on a TA Q500 model from TA Instruments by heating samples in alumina pans at a rate of 10 °C min^{-1} from 25 to 600 °C in a nitrogen flow and from 600 to 800 °C in air. Change of the gas at 600 °C was used to remove completely the carbonaceous residues from pyrolysis reactions and measure the exact organic residue amount.

Powder X-ray diffraction (XRD) patterns were collected on an X'Pert Pro Bragg Brentano diffractometer (PANalytical) using Cu Kα radiation (40 mA and 45 kV), with a scan speed of 0.01 °C min^{-1}. Gas-volumetric analysis, specific surface area (SSA), pore volume and size were measured by N_2 adsorption–desorption isotherms at 77 K using an ASAP 2020 (Micromeritics) gas-volumetric analyzer. SSA was calculated using the Brunauer–Emmett–Teller (BET) method; average pore size and volume were calculated on the adsorption branch of the isotherms according to the Barrett–Joyner–Halenda (BJH) method (Kruk–Jaroniec–Sayari equations). Samples were outgassed at RT overnight before analyses.

High resolution transmission electron microscopy (HRTEM) images were obtained with a JEOL 2010 instrument (300 kV) equipped with a LaB_6 filament. For specimen preparation powdery samples were supported onto hole carbon coated copper grids by dry deposition. Dynamic light scattering (DLS) measurements were carried out by using Malvern ZS 90 Zetasizer instrument. 0.1% suspensions of nanoparticles were prepared in deionized water and these suspensions were sonicated for 20 min before the analysis.

Synthesis of PNIPAM Homopolymers

Weighed quantity of monomer NIPAM was dissolved in dry ethanol in a single neck round-bottom flask equipped with a distillation apparatus, the solution of monomer was degassed for 10 min and then AIBN dissolved in dry ethanol was injected to the flask. The solvent from the flask was disttilled off under reduced pressure at 70 °C. The sticky mass of polymer obtained

Table I. List of Synthesized Poly(*N*-isopropylacrylamide)s

PNIPAM	NIPAM/AIBN mole ratio	M_w (Da)	M_n (Da)	Dispersity	Onset (°C)	LCST (°C)
1	10:1	33,600	14,400	2.3	30.8	31.2
2	20:1	60,100	20,300	2.9	30.7	31.1
3	30:1	78,900	27,000	2.9	30.6	31.0
4	40:1	86,400	26,400	3.2	30.5	30.9
5	50:1	148,700	39,700	3.7	30.7	31.0

was dissolved in acetone and reprecipitated from cold hexane. Reprecipitation was done twice. The polymer obtained was dried under vaccum. Five samples as reported in Table I were synthesized with varying mole ratio of NIPAM to AIBN.

Synthesis of MSNs

The synthesis of MSNs was carried out following the same procedure already reported elsewhere.[19,26,27] CTAB was used as cationic micelle forming templating agent, while TMB was used as the micelle core swelling agent. In a typical reaction CTAB (1 g) was dissolved in water (480 mL) then NaOH (3.5 mL, 2 *M*) was added and the solution was heated at 80 °C. After stabilization of the temperature, a proper amount of 1,3,5-trimethylbenzene was added to the system. The mixture was stirred for 30 min for the formation of a stable white emulsion. TEOS (5 mL) was added drop wise. The mixture was then stirred for 2 h at 80 °C. After cooling to room temperature, the powder product was isolated by filtration, washed with distilled water and methanol, and air-dried for 24 h. The as-synthesized material was then calcinated at 550 °C for 7 h in air (2 °C/min from room temperature to 550 °C in nitrogen and then isothermally at 550 °C in air).

Synthesis of MSNs-MPS Nanoparticles

MSNs (280 mg) were taken in a single neck round-bottom flask and to it 10 mL of toluene was added. Then 25 μL of MPS was injected to the suspension. The suspension was sonicated for 15 min. The flask was then equipped with a condenser and the suspension was refluxed for ~16 h at 125–130 °C under nitrogen. At the end of the reaction toluene was separated from the particles by centrifugation. The nanoparticles were washed two times with ~3 mL of fresh toluene and then with 5 mL of ethanol to remove excess and physically adsorbed MPS. The particles were then dried in air and characterized.

Grafting of PNIPAM on MSNs

MSNs-MPS (50 mg) were taken in a 50 mL capacity single neck round-bottom flask, to it weighed quantity of NIPAM (50 mg), 20 mL of dry ethanol, and 7.2 mg AIBN initiator were added.

Table II. Grafting of PNIPAM on MSNs

MSNs-PNIPAM	MSNs-MPS/NIPAM weight ratio	NIPAM/AIBN mole ratio	Distilled EtOH (mL)	Grafting (wt %)
MP1	1:1	10:1	8	1
MP2	1:1	10:1	12	3
MP3	1:1	10:1	17	7
MP4	1:1	10:1	20	20

The suspension was sonicated for 10 min and then heated to 70–80 °C. Then measured quantity of ethanol was distilled off from the flask under reduced pressure. After distillation of the desired quantity of ethanol from the flask the heating was continued for ~20 min. Then the obtained milky suspension of PNIPAM-grafted MSNs was cooled and centrifuged to recover the polymer grafted particles. The particles were washed twice with 3 mL ethanol to remove unattached polymer and other impurities and then dried in air. Four samples as listed in Table II were synthesized.

RESULTS AND DISCUSSION

Synthesis of PNIPAMs

In DPP, a suitable solvent is the one which solubilizes completely the monomers and the initiator and will be a non-solvent for the polymer formed, hence the term precipitation is used in the name of this technique.[15] Acetonitrile is found to fulfill this requirement and it is used frequently for DPP of vinyl monomers.[18,20] Use of acetonitrile works well for the synthesis of microspheres of polymers and to obtain very high M_w polymers. However as the aim of this work was to obtain PNIPAM homopolymers with low or moderate M_w; ethanol was used as the solvent for the synthesis of PNIPAMs. The radical chain transfer reactions with the solvent help to obtain low or moderate M_w homopolymers. This control on M_w was desired due to two main reasons: first is to obtain PNIPAMs with different M_w to study the effect of M_w on LCST and second as the ultimate aim of the work is to graft PNIPAM inside the mesopores of MSNs in order to modulate their capability of hosting molecules by thermal stimuli, while high molecular weight polymers would completely block the pores by fully occupying the pore volume. As reported in Table I five PNIPAM homopolymer samples with varying ratios of AIBN initiator with NIPAM were synthesized and, as expected from the general dependence of the degree of polymerization from the monomer to initiator ratio in radical chain polymerization,[28] M_w was found to increase from 33,600 to 148,700 Da with decrease in the amount of initiator.

The ATR-FTIR spectra of NIPAM monomer and PNIPAMs 1–5 are shown in Figure 1. The spectrum of NIPAM shows an important peak due to C=C stretching at 1620 cm^{-1} which disappears upon polymerization. Its disappearance is not that evident as upon polymerization a new broad peak appears around 1638 cm^{-1} due to amide carbonyl group stretching. Each spectrum of PNIPAM 1–5 clearly showed the main characteristic peaks of the polymer at 1459, 1536, and 1638 cm^{-1} which are attributed to $-CH_3$ (bend.), C–N (stretch.), and C=O (stretch.),

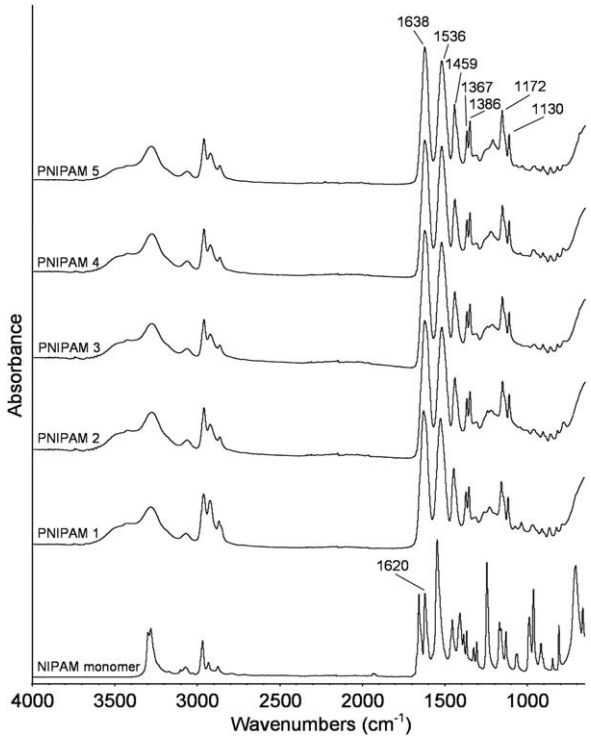

Figure 1. ATR-FTIR spectra of monomer NIPAM and PNIPAM homopolymers 1–5.

respectively.[29] The formation and structure of the polymer was further confirmed by ^{1}H-NMR spectroscopy. The NMR spectrum of PNIPAM 1 is illustrated in Figure 2 which shows the assignment of proton signals according to the polymer structure shown in the inset of the figure.[30,31] A representative TGA curve of homopolymer PNIPAM 3 is shown in Supporting Information Figure S1 and is characterized by a weight loss of ~14% due to the loss of water up to 100 °C and complete degradation of the polymer between 390 and 450 °C.

Transition of PNIPAM from the hydrophilic coil form to the relatively hydrophobic globule form is governed by various factors such as M_w, concentration, and end groups.[4,8] LCST and onset temperatures of synthesized PNIPAMs 1–5 were determined by DSC and are enlisted in Table I. It can be seen that a slight decrease of LCST was observed with increase in the M_w of the polymers. This slight decrease is attributed to the reduced entropy of mixing of the polymer chains with increased chain length.[4,8] PNIPAM 5 being the sample with high dispersity has not followed the order of decrease of transition temperature and its LCST is at 31 °C. The dispersity of polymers is found to increase with decreasing amount of the initiator. The role of dispersity in varying the LCST cannot be neglected as PNIPAM samples of the same molecular weights prepared by different polymerization techniques with different dispersity can have different LCST. It also depends upon the predominant presence of long or small polymer chain fractions in the sample. DSC curves of PNIPAMs 1–4 in Figure 3 showed the endothermic transitions at LCST of the polymers.

Synthesis of MSNs and PNIPAM Grafting

MSNs used in this work were synthesized by sol–gel synthesis method.[26,27] Quasi-spherical particles with hexagonal pore channels were obtained. The average size of the particles was 100–

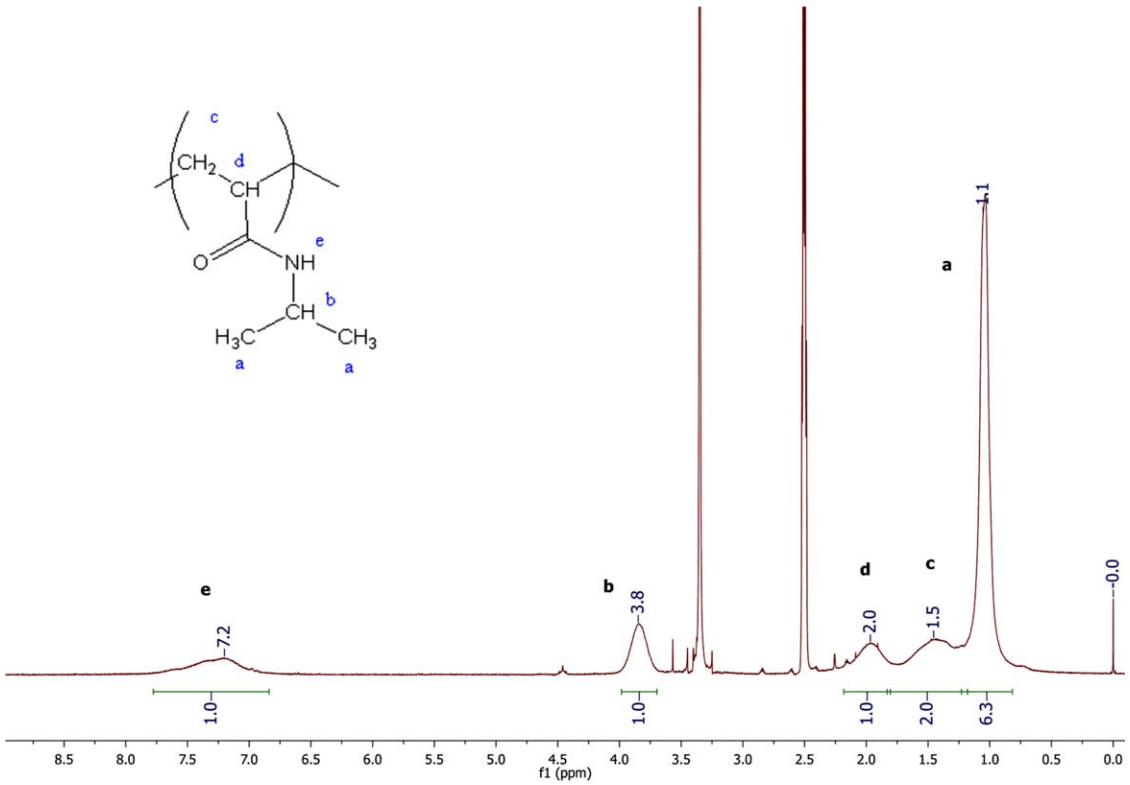

Figure 2. ^{1}H-NMR spectrum of PNIPAM 1 in DMSO-d_6. [Color figure can be viewed in the online issue, which is available at wileyonlinelibrary.com.]

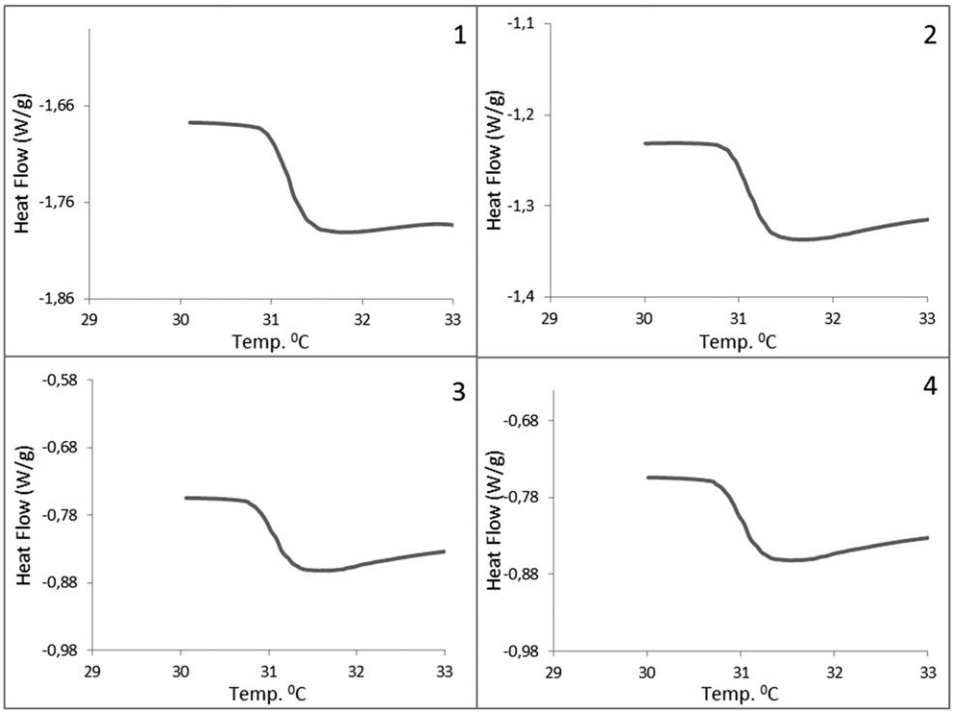

Figure 3. DSC curves of PNIPAM 1–4 from Table I showing LCSTs.

110 nm. Additional structural characterizations of particles were carried out by X-ray diffraction (XRD) and nitrogen adsorption–desorption analyses. The XRD spectrum of MSNs (Supporting Information Figure S2) confirmed the typical hexagonal pore channel structure with long range order. The SSA of particles calculated by Brunauer-Emmet-Teller (BET) method was 1021 m^2/g, cumulative pore volume was 2.42 m^2/g, and the pore diameter was 4.9 nanometers (Supporting Information Table S1). This pore size was tuned purposely so as to extend potential applications of the PNIPAM grafted porous particles prepared. Due to the sufficiently big pore size large drug molecules, fluorescent indicators (dyes) and also biomolecules can be loaded inside the mesopores of the silica particles used. A two-step synthetic procedure used for the grafting of PNIPAM on MSNs is depicted in Scheme 1.

First MSNs were functionalized with polymerizable acryloxy groups (MPS monomer) by the alkoxysilane grafting protocol.[32] MPS being a small organic molecule diffuses easily inside the mesopores of silica. Its grafting inside the mesopores in the first step guarantees the preferential grafting of PNIPAM inside the mesopores in the polymerization reaction. In the second step DPP of NIPAM in the presence of MSNs-MPS was carried out in ethanol by using AIBN as the initiator. The monomer to initiator ratio was 10:1, same as that used for the synthesis of homopolymer PNIPAM 1 from Table I. This ratio was chosen to obtain a polymer with similar M_w, LCST, and other properties as that for PNIPAM 1. The moderate M_w polymer formed in the presence of the particles gets grafted preferentially inside the mesopores of the nanoparticles than on its surface. The starting concentrations of NIPAM and AIBN in ethanol were 2.5 mg/mL and 0.36 mg/mL, respectively. Grafted quantity of polymers (quantitative grafting) is of great importance both in case of solid and mesoporous particles. In case of solid particles the amount of polymer grafted on the surface of particles determines the polymer shell thickness in the core–shell nanoparticles.[33] While in the case of mesoporous particles the amount of polymer grafted inside the pores is directly related to the decrease in pore volume. Hence precise control on the quantity of the grafted polymer is necessary.[19] One of the possible ways to tune the quantity of grafted polymer is to change the

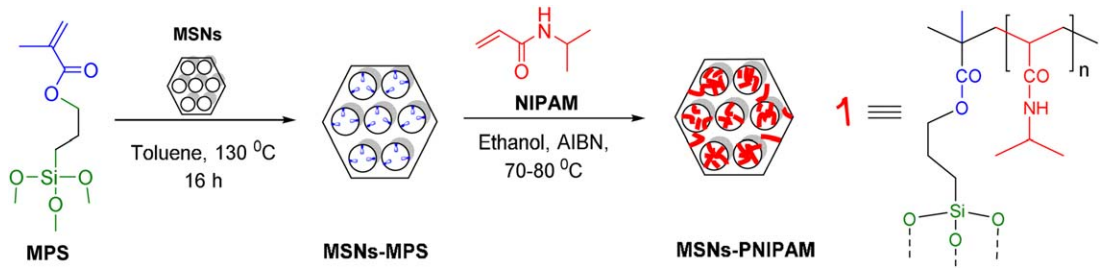

Scheme 1. Two step post-synthesis grafting of PNIPAM on mesoporous silica. [Color figure can be viewed in the online issue, which is available at wileyonlinelibrary.com.]

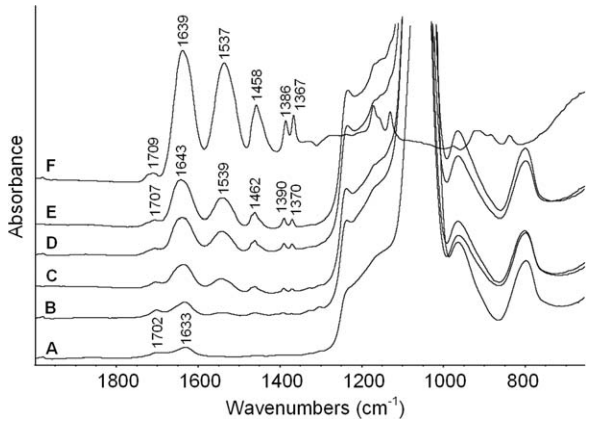

Figure 4. ATR-FTIR spectra of MSNs-MPS (A), MSNs-PNIPAM MP1-4 (B–E) and (F) Poly(NIPAM-co MPS).

monomer to particle ratio but it may not be feasible in certain cases. In this work it is shown that the other possible method to control quantitative grafting and which is feasible with DPP is to adjust the concentration of the reaction mixture by distilling out the solvent used for polymerization. As reported in Table II, by distilling out measured quantities of ethanol and by changing the starting concentrations of NIPAM (2.5 mg/mL) and AIBN (0.36 mg/mL) in the reaction mixture it was observed that the quantitative grafting of polymer can be changed. This observation therefore is of importance where change in monomer to particle ratio is not feasible to tune the quantitative grafting for practical reasons. Additionally as ethanol is one of the best solvents for PNIPAM, the non-grafted polymer chains remain in solution and the obtained hybrid nanoparticles are free from physisorbed polymer chains. The grafting of the PNIPAM on MSNs was confirmed by ATR-FTIR spectroscopy. The results obtained are shown in Figure 4 which shows ATR-FTIR spectra of MSNs-MPS and MSNs-PNIPAM samples MP1 to MP4.

The spectrum of MSNs-MPS showed two peaks at 1633 and 1702 cm^{-1} due to C═C stretching and carbonyl stretching from the acryloxy group. The PNIPAM grafted samples (B–E) showed the characteristic absorption peaks of the polymer. Twin peaks of C—H bending coming from the isopropyl group were observed at 1370, 1390 cm^{-1}. Additional characteristic peaks of the polymer at 1462, 1539 and 1643 cm^{-1} are attributed to —CH_3 (bend.), C—N (stretch.), and C═O (stretch.), respectively.[29] The carbonyl stretching peak at 1702 cm^{-1} from the acryloxy group is present in the PNIPAM grafted MSNs samples which is shifted to 1707 cm^{-1} upon polymerization (refer to the structure of grafted PNIPAM in Scheme 1). An increase in the intensities of PNIPAM peaks with increase in grafting was observed. Quantitative grafting of PNIPAM on MSNs was determined by TGA and the results are shown in Figure 5. Bare MSNs showed only 1% weight loss upon programmed heating up to 800 °C. MPS-grafted MSNs showed a weight loss of 10% indicating 9% by weight grafting of MPS. Instead PNIPAM-grafted MSNs samples MP1–MP4 showed 11, 13, 17, and 30% weight loss, respectively. The results of quantitative grafting by TGA are shown in Table II. TEM images of the bare (as such synthesized) and PNIPAM grafted particles are shown in Figure 6 (right side) and (left side) respectively, which confirmed that polymer grafting by DPP does not affect the stability of the particles and the pore structure. This observation was further supported by the nitrogen adsorption–desorption analyses (Supporting Information Table S1). The SSA of bare particles was changed from 1021 m^2/g to 662 m^2/g for the highest quantity (20%) of PNIPAM grafted sample MP4. While the pore diameters and pore volumes were changed from 4.9 nm to 4.3 nm and 2.42 to 1.06 cm^3/g, respectively. This data confirmed the grafting of PNIPAM inside the mesopores of the silica nanoparticles. So in comparison with other classical polymerization and grafting techniques for PNIPAM, the DPP technique provides an additional advantage of tuning quantitative grafting by manipulating the *in situ* polymerization reaction conditions.

DLS analysis of MP4 sample with 20% PNIPAM grafting was carried out. The particle size distributions of the sample at 25 °C and at 40 °C are shown in Figure 7. The transition of the PNIPAM chains grafted on the surface of the MSNs from extended coils to collapsed globules above LCST of PNIPAM

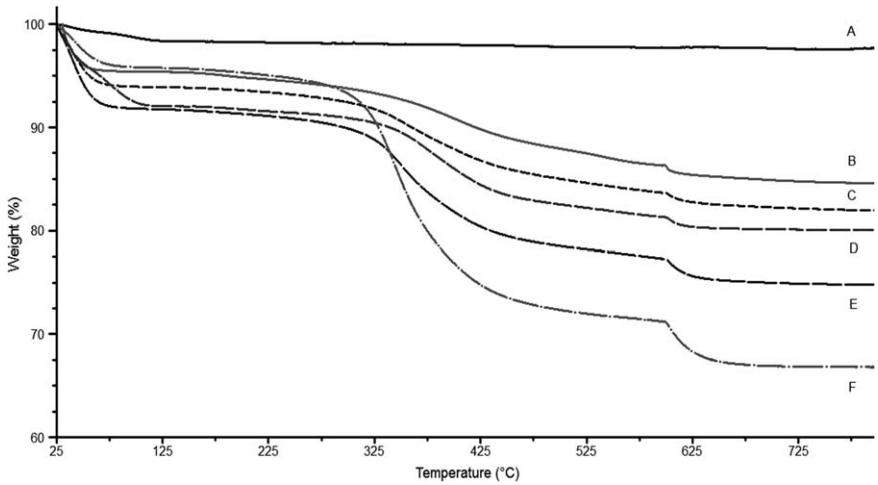

Figure 5. TGA curves of MSNs (A), MSNs-MPS (B), and MSNs-PNIPAM MP1 to MP4 (C–F respectively).

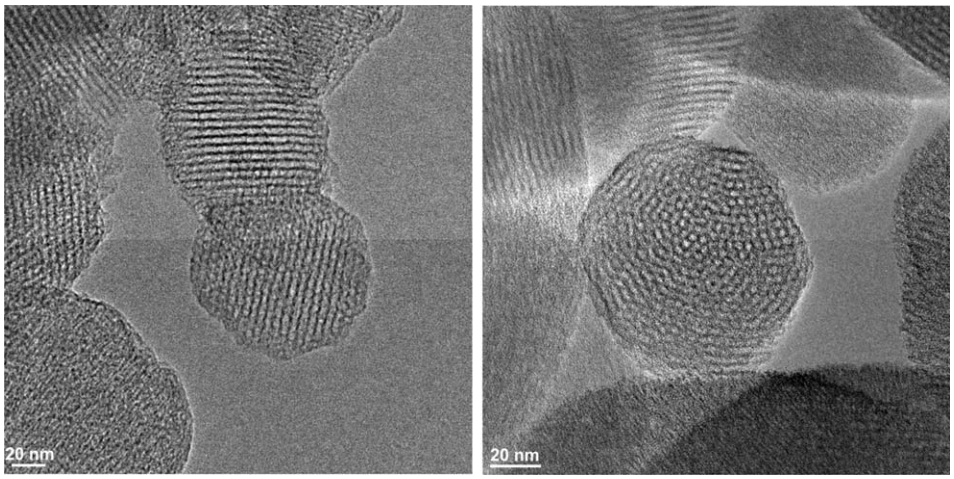

Figure 6. TEM images of bare (left) and MSN-PNIPAM (MP4) sample (right).

was clearly evident as the average hydrodynamic diameter (HD) of the hybrid particles at 25 °C was 164 nm which at 40 °C was decreased to 122 nm due to the shrinkage of PNIPAM chains on the surface of the particles.[34] The zeta potential values for bare MSNs and PNIPAM-grafted MSNs were −39.1 mV and −34.1 mV respectively, indicating slight reduction of free silanols upon polymer grafting. These results confirmed PNIPAM grafting and its thermoresponsive behavior on the surface of the MSNs.

CONCLUSIONS

In this work, PNIPAMs with different molecular weights were synthesized by DPP technique and fully characterized. Effect of M_w on LCST of PNIPAM homopolymers was reconfirmed as LCST of the polymers was slightly decreased with increase in M_w. In the two-step post-synthesis grafting procedure of PNIPAM on MSNs by DPP technique, it is showed that quantitative grafting of the polymer can be tuned by adjusting the concentration of monomer and initiator in the reaction mixture by distilling out a measured quantity of the solvent used for the polymerization reaction. By keeping constant the MSNs to monomer ratio the grafting of PNIPAM on MSNs was tuned from 1 to 20 by weight. Thus synthetic improvement and *in situ* control over the quantitative grafting of PNIPAM on porous silica nanoparticles was achieved. This observation is of importance to synthesize various composite and hybrid polymer-grafted nanoparticles with desired quantitative grafting of PNIPAM or its copolymers for various applications.

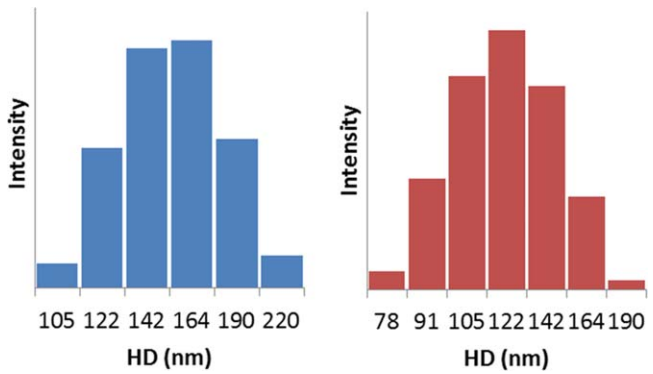

Figure 7. Average hydrodynamic diameters of MSNs-PNIPAM (MP4) sample at 25 °C (blue/left) and 40 °C (red/right). [Color figure can be viewed in the online issue, which is available at wileyonlinelibrary.com.]

ACKNOWLEDGMENTS

The Marie Sklodowska-Curie Research and Innovation Staff Exchange project funded by the European Commission H2020-MSCA-RISE-2014 within the framework of the research project Mat4treaT (Project number: 645551) is acknowledged. This work was supported by the European COST Action MP1202 "Rational design of hybrid organic inorganic interfaces: the next step towards advanced functional materials". Dr. S. A. Jadhav thank MIUR Italy for financial support. The authors thank Dr. P. Quagliotto for NMR analysis.

REFERENCES

1. Heskins, M.; Guillet, J. E. *J. Macromol. Sci. A* **1968**, *2*, 1441.
2. Schild, H. G. *Prog. Polym. Sci.* **1992**, *17*, 163.
3. Halperin, A.; Kroger, M.; Winnik, F. M. *Angew. Chem. Int. Ed.* **2015**, *54*, 15342.
4. Xia, Y.; Yin, X.; Burke, N. A. D.; Stover, H. D. H. *Macromolecules* **2015**, *38*, 5937.
5. Yim, H.; Kent, M. S.; Mendez, S.; Lopez, G. P.; Satija, S.; Seo, Y. *Macromolecules* **2006**, *39*, 3420.
6. Jhon, Y. K.; Bhat, R. R.; Jeong, C.; Rojas, O.; Szleifer, I.; Genzer, J. *Macromol. Rapid. Commun.* **2006**, *27*, 697.
7. Zhang, Y.; Furyk, S.; Sagle, L. B.; Cho, Y.; Bergbreiter, D. E.; Cremer, P. S. *J. Phys. Chem. C* **2007**, *111*, 8916.
8. Furyk, S.; Zhang, Y.; Ortiz-Acosta, D.; Cremer, P. S.; Berbreiter, D. E. *J. Polym. Chem. A* **2006**, *44*, 1492.
9. Brunella, V.; Jadhav, S. A.; Miletto, I.; Berlier, G.; Ugazio, E.; Sapino, S.; Scalarone, D. *React. Func. Polym.* **2016**, *98*, 31.

10. Ilic-Stojanovic, S.; Nikolic, L.; Nikolic, V.; Ristic, I.; Budinski-Simendic, J.; Kapor, A.; Nikolic, G. M. *Polym. Int.* **2014**, *63*, 973.
11. Qiao, X.; Zhang, Z. *J. Photochem. Photobiol. A* **2007**, *190*, 15.
12. Bathfield, M.; Reboul, J.; Cacciaguerra, T.; Lacroix-Desmazes, P.; Gerardin, C. *Chem. Mater.* **2016**, *28*, 3374.
13. Liu, C.; Guo, J.; Yang, W.; Hu, J.; Wang, C.; Fu, S. *J. Mater. Chem.* **2009**, *19*, 4764.
14. Li, G. J.; Mohwald, H.; Shchukin, D. G. *Chem. Soc. Rev.* **2012**, *42*, 3628.
15. Bai, F.; Huang, B.; Yang, X.; Huang, W. *Eur. Polym. J.* **2007**, *43*, 3923.
16. Zhang, D.; Liu, J.; Liu, T.; Yang, X. *Colloid Polym. Sci.* **2015**, *293*, 1799.
17. Li, G.; Kang, E. T.; Neoh, K. G. *Langmuir* **2009**, *25*, 4361.
18. Effati, E.; Pourabbas, B. *Powder Technol.* **2013**, *1*, 473.
19. Jadhav, S. A.; Miletto, I.; Brunella, V.; Berlier, G.; Scalarone, D. *Polym. Adv. Technol.* **2015**, *26*, 1070.
20. Zhang, X.; He, X.; Chen, L.; Zhang, Y. *J. Mater. Chem. B* **2014**, *2*, 3254.
21. Shao, Y.; Zhou, L.; Bao, C.; Maa, J.; Liu, M.; Wang, F. *Chem. Eng. J.* **2016**, *283*, 1127.
22. Liu, J.; Li, L.; Tang, H.; Zhao, F.; Ye, B. C.; Li, Y.; Yao, J. *J. Sep. Sci.* **2015**, *38*, 3103.
23. Liu, J.; Zhang, L.; Li, L.; Song, H.; Liu, Y.; Tang, H.; Li, Y. *J. Sep. Sci.* **2015**, *38*, 1172.
24. Liu, J.; Yang, K.; Qu, Y.; Li, S.; Wu, Q.; Liang, Z.; Zhang, L.; Zhang, Y. *Chem. Commun.* **2015**, *51*, 3896.
25. Guisasola, E.; Baeza, A.; Talelli, M.; Arcos, D.; Vallet-Regi, M. *RSC Adv.* **2016**, *6*, 42510.
26. Jana, S. K.; Mochizuki, A.; Namba, S. *Catal. Surv. Asia* **2004**, *8*, 1.
27. Peng, J.; Liu, J.; Yang, Y.; Li, C.; Yang, Q. *J. Mater. Chem. A* **2014**, *2*, 8118.
28. Odian, G. Principles of Polymerization, 4th ed.; Wiley: Hoboken, New Jersey, **2004**.
29. Katsumoto, Y.; Tanaka, T.; Sato, H.; Ozaki, Y. *J. Phys. Chem. A* **2002**, *106*, 3429.
30. Sun, S.; Wu, P.; Zhang, W.; Zhang, W.; Zhu, X. *Soft Matter* **2013**, *9*, 1807.
31. Schonhoff, M.; Larsson, A.; Welzel, P. B.; Kuckling, D. *J. Phys. Chem. B* **2002**, *106*, 7800.
32. Jadhav, S. A.; Brunella, V.; Scalarone, D. *Part. Part. Syst. Character.* **2015**, *32*, 417.
33. Zhang, K.; Chen, H.; Chen, X.; Chen, Z.; Cui, Z.; Yang, B. *Macromol. Mater. Eng.* **2003**, *288*, 380.
34. Walldal, C.; Wall, S. *Colloid Polym. Sci.* **2000**, *278*, 936.